International Journal of Nanomedicine

Dovepress
open access to scientific and medical research

Open Access Full Text Article

ORIGINAL RESEARCH

Silk Fabrics Modified with Photothermal Phase Change Microcapsules for Personal Thermal Management

Gang Deng, Yuanyuan Yang, Song Lu, Lin Ma, Guohua Wu

College of Biotechnology and Sericultural Research Institute, Jiangsu University of Science and Technology, Zhenjiang, 212100, People's Republic of China

Correspondence: Guohua Wu, Email ghwu@just.edu.cn

International Journal of Nanomedicine downloaded from https://www.dovepress.com/
For personal use only.

Introduction: With the development of technology, personal heat management has become a focus of attention. Phase change fabrics, as intelligent materials, are expected to be widely used in multiple fields, bringing comfortable, intelligent and convenient living experience.

Methods: In this study, miniature phase change microcapsules (MPCM) with n-octadecane as core and poly(methyl methacrylate) as shell were successfully prepared. Using the in-situ reduction property of polydopamine, gold nanoparticles were deposited on the surface of the microcapsules, which retained the heat storage function and imparted photothermal and antibacterial properties. The MPCM with photothermal conversion function was modified on the surface of silk fabric using aqueous polyurethane after verified by comprehensive material characterisation techniques.

Results: Under the near infrared light of 808 nm wavelength and 0.134 W/cm² irradiation intensity, the MPCM@PDA@Au modified silk fabrics showed excellent photothermal conversion performance, which could be increased from 25°C to 60°C in 50s. After the light source was cut off, the fabrics showed good heat release ability, with melting enthalpy and crystallisation enthalpy reaching 41.58 J/g and 43.3 J/g, respectively, which were not changed after repeated cycles. After the light source is cut off, the fabric has good heat release ability, and the enthalpy of melting and crystallisation reaches 41.58 J/g and 43.3 J/g, respectively, and the photothermal efficiency remains unchanged after many cycles of use, which proves that it has excellent durability and stability. The antimicrobial test shows that the fabric has significant antibacterial effect on Escherichia coli (E. coli) and Staphylococcus aureus (S. aureus).

Discussion: MPCM@PDA@Au silk fabrics bring new possibilities for the future of personal thermal management and antimicrobial protection in the field of medical health, outdoor sports and other areas of broad application prospects, heralding the birth of a series of innovative applications and solutions.

Keywords: photothermal conversion, phase change material, thermal energy storage, functional textile

Introduction

As living environments and working conditions continue to improve, personal thermal management is receiving increasing attention.[1–3] The significance of factors such as temperature and humidity on human health has been widely acknowledged. Both excessively high and low temperatures can adversely affect human health, making personal thermal management an integral part of modern life.[4,5] In this context, phase change fabrics, with their notable characteristics of being lightweight, energy-efficient, environmentally friendly, and intelligent, are gradually gaining widespread recognition and favor.[6,7] Phase change fabric is an intelligent fabric material that incorporates phase change capsule technology modified on the fabric surface, enabling it to regulate the temperature of the surrounding environment by absorbing or releasing heat.[8] This innovative fabric material has a wide range of applications. For instance, in cold winter weather, wearing phase change fabric clothing can keep individuals comfortable and warm outdoors, while in hot summer conditions, it can help maintain a comfortable body temperature even in high outdoor temperatures.[9–11] In conclusion, phase change fabrics, as a highly promising intelligent material, are expected to find widespread use in various fields in

Received: 23 May 2024
Accepted: 31 July 2024
Published: 20 August 2024

© 2024 Deng et al. This work is published and licensed by Dove Medical Press Limited. The full terms of this license are available at https://www.dovepress.com/terms.php and incorporate the Creative Commons Attribution – Non Commercial (unported, v3.0) License (http://creativecommons.org/licenses/by-nc/3.0/). By accessing the work you hereby accept the Terms. Non-commercial uses of the work are permitted without any further permission from Dove Medical Press Limited, provided the work is properly attributed. For permission for commercial use of this work, please see paragraphs 4.2 and 5 of our Terms (https://www.dovepress.com/terms.php).

the future, providing people with a more comfortable, intelligent, and convenient living experience. The availability of abundant and sustainable solar energy further supports the successful application of photothermal conversion for personal thermoregulation.

Solar energy is an inexhaustible energy source with the advantages of economy, environmental protection, and safety. It is expected to replace traditional fossil energy as one of the most promising energy sources in the future.[12,13] However, the effective utilization of solar energy is limited by its intermittent and random nature.[14] To address this issue, a storage medium that can store excess energy and release it when needed is required. Phase change materials possess excellent thermal storage properties that meet this requirement.[15] Unfortunately, conventional phase change materials suffer from poor solar energy capture capability, resulting in low solar energy utilization. Therefore, combining photothermal materials and phase change materials is an effective strategy for efficient solar energy utilization.[16–18] For instance, Sun et al synthesized n-docosane@SiO_2 phase change microcapsules by interfacial polycondensation. They then deposited a PDA layer on the surface of the SiO_2 shell through in-situ oxidative polymerization and chemically grafted CNTs onto the PDA layer. This CNTs/PDA coating effectively traps photons, endowing the microcapsules with efficient solar-thermal energy conversion. The phase transition enthalpy of these microcapsules exceeded 130.0 J/g, and the photothermal conversion efficiency reached 90.1%.[19] Similarly, Wu et al found that the temperature of PDA-deposited n-octadecane@SiO_2 microcapsules was higher than that of non-PDA-deposited microcapsules for the same irradiation time, with the photothermal conversion efficiency increasing from 18.6% to 91.8%.[20] Gao et al prepared octadecane@-melamine formaldehyde resin phase change microcapsules by in-situ polymerization, with shells modified by reduced graphene oxide and cores doped with oleic acid-coated Fe_3O_4 magnetic nanoparticles. These hybridized phase change microcapsules achieved the combined functions of photothermal conversion, phase change energy storage, and magnetic controllability.[21] The photothermal conversion phase-change microcapsules addressed the common issue of low solar energy utilization in phase-change microcapsules and possessed heat storage and exothermic properties compared to photothermal materials.[22,23] The application of photothermal phase change capsules in the textile field is highly significant, providing new possibilities for the functional expansion of textiles. With the continuous advancement of photothermal phase change capsule preparation technology, its application in the textile field will become more extensive.[16,24]

Silk, derived from nature, is renowned for its lustrous white hue, exceptional skin-friendliness, remarkable moisture absorption capabilities, and heat resistance. Its fibre properties closely resemble those of human skin, offering a soft and delicate touch that provides an ultimate comfort experience. Silk efficiently absorbs and disperses moisture from the skin's surface, keeping it dry and mitigating skin issues associated with sweat accumulation. Furthermore, silk exhibits heat resistance, remains stable in high-temperature environments, and is resistant to deformation or damage. Notably, silk is also affordably priced, with its products widely popular, enabling a broader range of individuals to easily embrace this natural gift.[25–28]

In this study, we cleverly integrated the unique advantages of phase change materials, photothermal materials and silk, and successfully synthesised a MPCM by using n-octadecane as the core and poly(methyl methacrylate) (PMMA) as the shell material. Subsequently, the polymerisation reaction of dopamine on the surface of MPCM was induced under a weakly alkaline environment, resulting in the formation of a polydopamine film. Notably, the surface of polydopamine is rich in phenolic hydroxyl functional groups and exhibits good reducing properties.[29] In order to further enhance its functionality, a layer of gold nanoparticles was deposited on the surface of MPCM@PDA by taking advantage of the reducing property of polydopamine, thus constructing the MPCM@PDA@Au multilayer core-shell structure. Thereafter, waterborne polyurethane (WPU) was employed as a medium to modify this photothermal phase change capsule with multifunctionality onto the silk surface. This innovative strategy not only endows silk fabrics with photothermal capability, but also with multiple functions such as heat storage, temperature regulation, and bacterial inhibition. By simply regulating the light conditions, the temperature of the silk fabric can be effectively regulated to achieve the effect of photothermal. At the same time, MPCM's efficient heat storage performance allows it to absorb or release heat, which helps maintain a constant temperature of silk fabrics. In addition, the bacteriostatic properties of the MPCM@PDA@Au multilayered core-shell structure add extra bacteriostatic functions to the silk fabric. In summary, we have successfully endowed silk fabrics with multiple functions by modifying low-cost and cost-effective functional photothermal phase

change capsules on the surface of silkworms, and this innovative approach demonstrates the potential for a wide range of applications in the textile field.

Results and Discussion

We conducted exhaustive microstructural tests on MPCM, MPCM@PDA, and MPCM@PDA@Au to probe deeply into their internal structure. Firstly, the MPCM was carefully observed using scanning electron microscopy (SEM) and transmission electron microscopy (TEM). The SEM images (Figure 1A) clearly demonstrate the successful synthesis of MPCM with a particle size of about 10 μm. These capsules presented a complete structure and smooth surface, highlighting the high quality of preparation. TEM results (Figure 1B) further revealed the internal details of the MPCM capsules, showing that phase change capsule particles formed from n-octadecane were successfully encapsulated inside the MPCM. Then, the same test was performed for MPCM@PDA. SEM images (Figure 1C) showed that the surface of the capsule was covered with a layer of dark material, which was the result of PDA deposition. The TEM image (Figure 1D), on the other hand, demonstrated the folded structure formed by the PDA layer on the surface of the MPCM capsule. Subsequently, the MPCM@PDA@Au was tested by SEM and TEM. The SEM images (Figure 1E) of MPCM@PDA@Au did not show much morphological changes. The TEM images (Figure 1F) showed that gold nanoparticles were generated in situ on the surface of the MPCM@PDA capsule and exhibited granular fabrication. Finally, after Energy Dispersive Spectrometer (EDS) test analysis (Figure 1H–J), it was known that the main constituent element of MPCM and MPCM@PDA after PDA encapsulation was carbon. Further, when the gold nanoparticle layer was generated in situ on the surface of MPCM@PDA, the EDS results clearly showed that the gold element occupied 27.98% of the content, which was a strong evidence of the successful loading of gold nanoparticles. The EDS image of MPCM@PDA@Au (shown in Figure 1G) visually demonstrated the homogeneous fabrication of the gold nanoparticles on the surface of the capsule, which further proved the reliability and homogeneity of the preparation method. In summary, we successfully prepared MPCM microcapsules with an average particle size of about 10 μm and sequentially modified PDA and gold nanolayers on their surfaces by layer-by-layer coating technique. These results not only validate the effectiveness of the

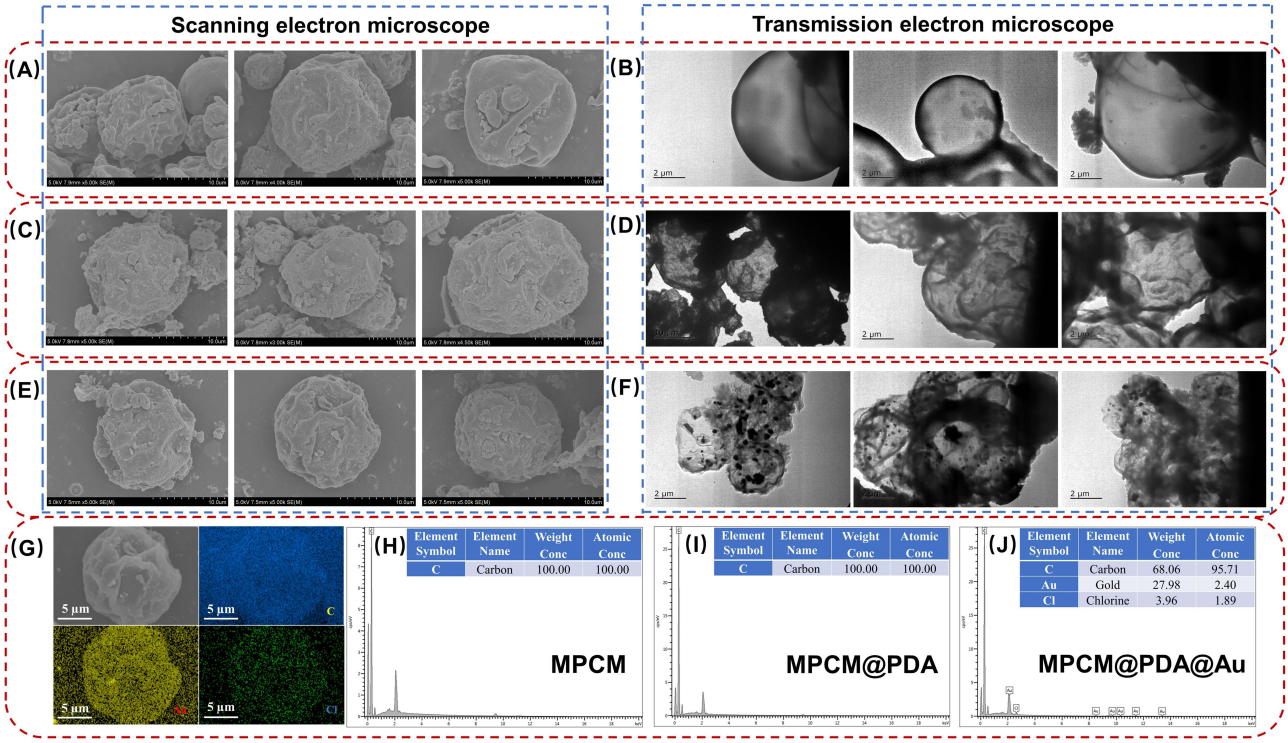

Figure 1 (**A**) SEM image of MPCM, (**B**) TEM image of MPCM. (**C**) SEM image of MPCM@PDA. (**D**) TEM image of MPCM@PDA. (**E**) SEM image of MPCM@PDA@Au. (**F**) TEM image of MPCM@PDA@Au. (**G**) EDS mapping of MPCM@PDA@Au. Additionally, (**H**), (**I**), and (**J**) show the EDS elemental analyses of MPCM, MPCM@PDA, and MPCM@PDA@Au, respectively.

preparation strategy, but also lay a solid foundation for an in-depth exploration of the performance of these functionalized microcapsules in phase change energy storage materials as well as other potential applications.

The compositional and structural properties of MPCM and its modified materials were deeply investigated by the combined analysis of FTIR and XRD. The FTIR (Figure 2A) clearly demonstrated that the MPCM consists of n-octadecane and PMMA, where the characteristic peaks at 2923 cm^{-1} and 2854 cm^{-1} corresponded to the

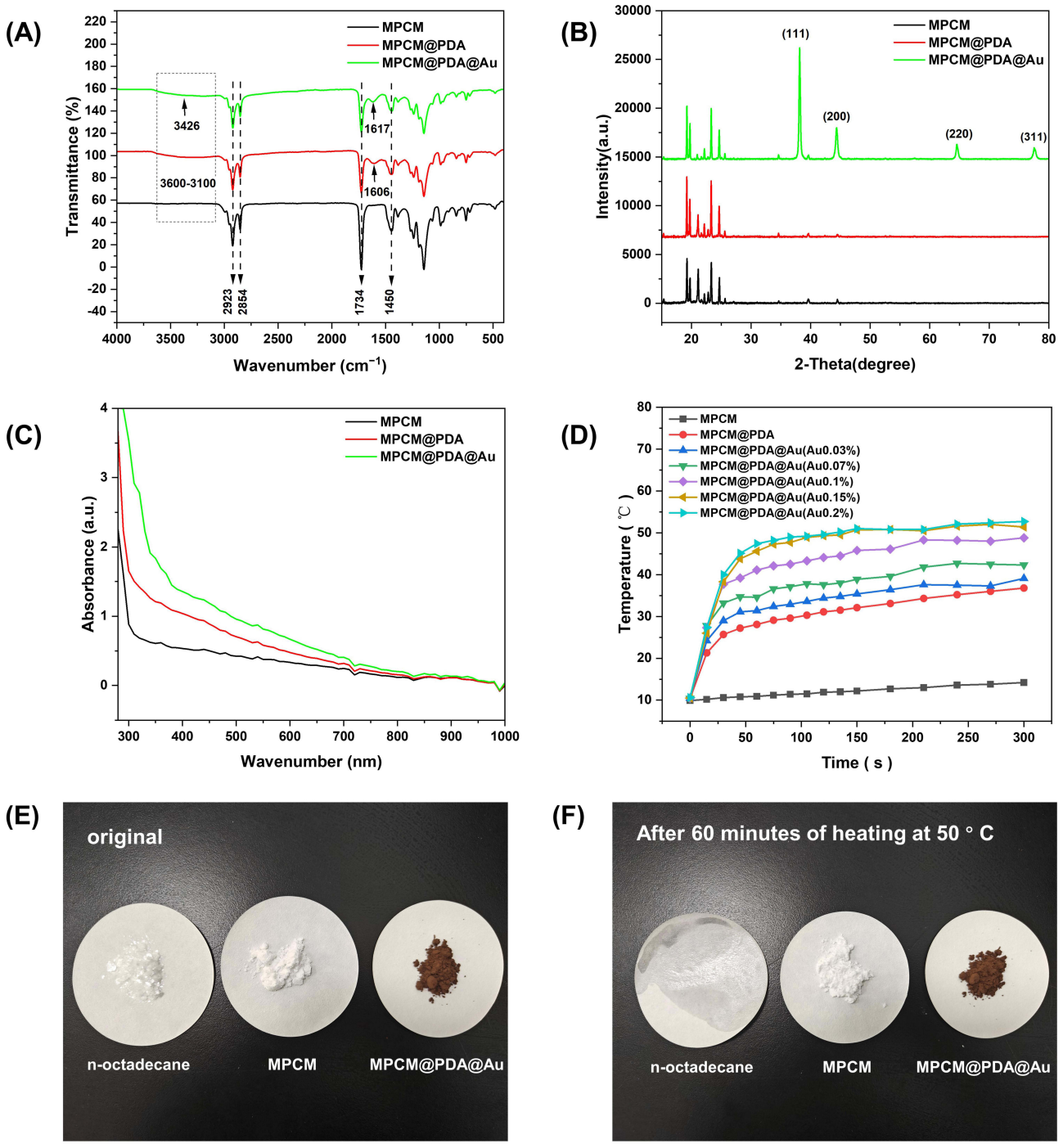

Figure 2 (**A**) FTIR spectra of MPCM, MPCM@PDA, and MPCM@PDA@Au. (**B**) XRD patterns of MPCM, MPCM@PDA, and MPCM@PDA@Au. (**C**) UV-Vis-NIR absorption spectra of MPCM, MPCM@PDA, and MPCM@PDA@Au. (**D**) Photothermal results of MPCM, MPCM@PDA, and MPCM@PDA@Au. (**E**) Optical images of the original morphology of n-octadecane, MPCM and MPCM@PDA@Au. (**F**) Optical images of the morphology of n-octadecane, MPCM and MPCM@PDA@Au after heating in an oven at 50°C for 60 min.

C-H stretching vibration of n-octadecane,[30,31] whereas the peak at 1734 cm^{-1} was the characteristic peak of the C=O bond in PMMA. Further observation of the peak at 1450 cm^{-1}, which is attributed to the bending vibration of the C-H bond in PMMA, again confirms the composition of MPCM.[32–34] When the MPCM surface was successfully encapsulated by dopamine, the FTIR presented new telescopic vibrational peaks in the range of 3100–3600 cm^{-1}, which were associated with the -OH and -NH_2 groups in the catechol moiety.[35] In addition, the peak at 1606 cm^{-1} corresponded to the aromatic ring backbone vibration, further confirming the successful modification of dopamine on the MPCM surface. Subsequently, gold nanoparticles were generated in situ on the MPCM@PDA surface. The IR spectra showed that the peak intensity of MPCM@PDA@Au in the range of 3100–3600 cm^{-1} was attenuated, while the peak at 1606 cm^{-1} was red-shifted to 1617 cm^{-1} and accompanied by a reduction in peak area. These changes were attributed to the interaction between the phenolic hydroxyl group in polydopamine and chloroauric acid, which led to the depletion of the phenolic hydroxyl group, resulting in the successful generation of gold nanoparticles on the MPCM@PDA surface.[36,37] This not only proves the successful loading of gold nanoparticles, but also reveals the interaction mechanism between polydopamine and gold nanoparticles. XRD analysis (Figure 2B) further supports our conclusion. The characteristic peaks of n-octadecane were clearly visible in the range of 11.52° to 44.58.[30] After encapsulation of dopamine, the XRD pattern of MPCM@PDA remained unchanged, indicating that its crystallinity was not affected. In contrast, when gold nanoparticles were generated in situ on the surface of MPCM@PDA, characteristic peaks corresponding to the crystalline faces of gold (111), (200), (220), and (311) appeared in the XRD pattern of MPCM@PDA@Au, confirming the successful generation of gold nanoparticles on the surface of MPCM@PDA.[38] In addition, the UV-Vis-NIR absorption spectra of the three materials in ethanol solution were determined (Figure 2C). The results showed that the absorbance of the materials in the UV band was gradually enhanced as the modification proceeded from MPCM to MPCM@PDA to MPCM@PDA@Au. This indicates that the gradual modification successfully enhanced the light absorption of the microcapsules in the UV band. Finally, the photothermal properties of MPCM, MPCM@PDA and MPCM@PDA@Au were also compared (Figure 2D). The pristine MPCM did not possess the photothermal ability, but the MPCM@PDA formed after encapsulating dopamine exhibited some photothermal conversion ability. When gold nanoparticles were further synthesised on the surface of MPCM@PDA, the photothermal performance of MPCM@PDA@Au was significantly enhanced, which was attributed to the excellent photothermal conversion efficiency of gold nanoparticles.[39] Additionally, as the gold concentration increases, the photothermal effect gradually intensifies until saturation. Through stepwise modification, not only is the phase change ability of the microcapsules retained, but they are also successfully endowed with photothermal conversion properties. In addition, in order to comprehensively evaluate the thermal stability of the deformation capsules and their anti-leakage performance under high-temperature environments, the samples of n-octadecane, MPCM, and MPCM@PDA@Au were placed in an oven and heated at 50 °C for 60 min, and they were carefully observed for any leakage phenomena. The results of the experiments (shown in Figure 2E and F). After heating at 50 °C for 60 min, the n-octadecane sample has completely melted, while no obvious signs of leakage are observed for both MPCM and MPCM@PDA@Au samples. This indicates that MPCM itself has good thermal stability and can effectively prevent the leakage of the contents within a certain temperature range. Meanwhile, the MPCM@PDA@Au samples also demonstrated comparable leakage prevention effects with MPCM. In summary, both MPCM and MPCM@PDA@Au showed excellent leakage prevention capability.

Observed by SEM, we can clearly see that the surface of the unmodified silk fabric presents a smooth feature (as shown in Figure 3A). However, when the silk fabric was modified by MPCM@PDA@Au, its surface morphology changed significantly and became rough and uneven (as shown in Figure 3B). In order to further verify the modification effect, the modified silk fabric was subjected to EDS characterisation (shown in Figure 3C). The EDS results showed that, in addition to the original carbon and oxygen elements, gold elements appeared, and the gold elements were uniformly distributed on the surface of the silk fabric. This indicates that MPCM@PDA@Au was successfully and uniformly modified on the surface of silk fabric. In order to compare the elemental changes before and after modification more intuitively, EDS elemental analyses were carried out on the blank silk fabric and the modified MPCM@PDA@Au silk fabric (shown in Figure 3D). By comparing the elemental contents of the two, it can be clearly found that the blank silk fabric contains only the elements of carbon and oxygen, while the element of gold does not exist. However, in the

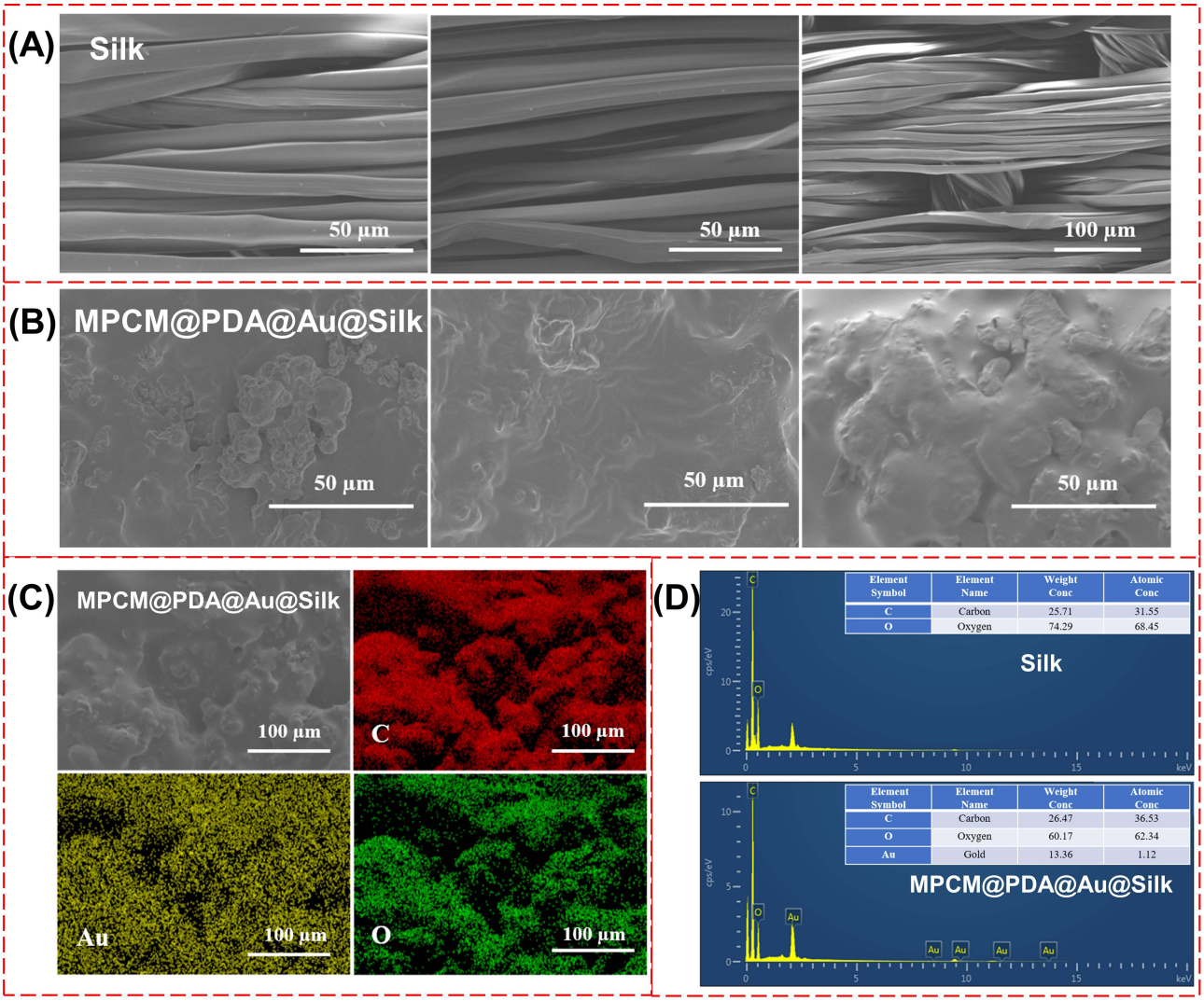

Figure 3 (**A**) SEM image of silk fabrics. (**B**) SEM image of MPCM@PDA@Au-coated silk fabrics. (**C**) EDS plot of the elemental composition of MPCM@PDA@Au silk fabrics. (**D**) a comparative EDS analysis between silk fabrics and MPCM@PDA@Au silk fabrics.

modified MPCM@PDA@Au silk fabrics, the signals of gold elements clearly appeared. This finding further confirms that MPCM@PDA@Au has been successfully modified onto the surface of silk fabrics.

After the successful modification of MPCM@PDA@Au on the surface of silk fabric, it was fully and exhaustively characterised. Specific absorption peaks were clearly observed by FTIR (as shown in Figure 4A). Specifically, the characteristic peaks of the unmodified silk fabric at 1648 cm^{-1} and 1527 cm^{-1} are attributed to the random curl in amide I and the β-folded structure in amide II band, respectively.[40] The peak at 2915 cm^{-1} is attributed to the C-H stretching vibration of n-octadecane,[31] which clearly points out its presence, while the peaks at 1727 cm^{-1} and 1241 cm^{-1} are correspond to the C=O stretching vibration and urethane stretching vibration of polyurethane, respectively, confirming the key role of polyurethane in the modification process.[41,42] No characteristic absorption peak belonging to -NCO was detected at 2270 cm^{-1}, which indicates that the isocyanate has been completely converted to a carbamate bond. It is possible that the isocyanate groups were polymerised with silk and MPCM@PDA@Au, and this reaction effectively enhanced the adhesion between MPCM@PDA@Au and silk. It is speculated that MPCM@PDA@Au may be firmly adhered to the surface of the silk fabric through chemical bonding and various other ways of interaction.[43,44] These FTIR data provide strong evidence for the successful anchoring of MPCM@PDA@Au to the surface of silk fabric via polyurethane. In addition, XRD analyses (shown in Figure 4B) further revealed the structural information of the surface

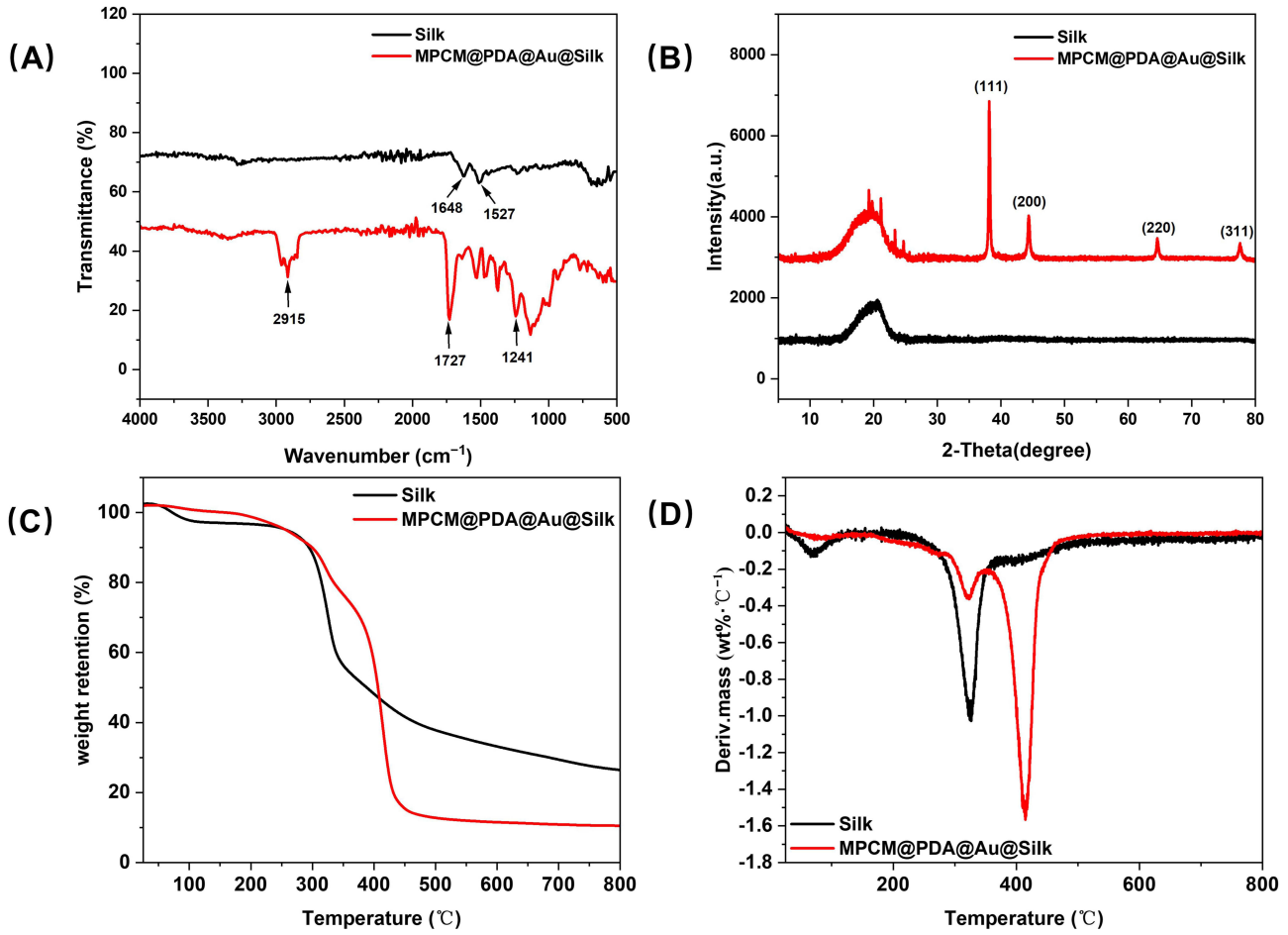

Figure 4 (**A**) FTIR spectra. (**B**) XRD patterns. (**C**) Thermogravimetric curves. (**D**) DTG plots of both plain silk fabrics and MPCM@PDA@Au-modified silk fabrics.

modification. The characteristic peak presented at ~20.6° in the original sample of silk fabric is a typical signature of silk material. In contrast, on the MPCM@PDA@Au-modified silk fabric, not only the characteristic peaks of silk were retained, but also new diffraction peaks appeared, which coincided perfectly with the (111), (200), (220) and (311) crystal planes of gold nanoparticles.[38] Particularly noteworthy is the observation of the characteristic peaks of n-octadecane in the range of 11.52° to 44.58,[30] which further confirms that MPCM@PDA@Au has been successfully and stably modified on the surface of silk fabrics, providing strong structural evidences for our study. Meanwhile, thermogravimetric (TG) and derivative thermogravimetric (DTG) analyses revealed the thermal stability of silk fabrics. The results are shown in Figure 4C and D. In the range of 40–130°C, there is a slight mass loss in silk fabrics due to water evaporation. And in the high temperature range of 240–480°C, thermal degradation of silk protein becomes the main cause of mass loss.[45] However, after modified with waterborne polyurethane and attached with MPCM@PDA@Au, the thermal stability of silk fabrics was significantly improved. In particular, in the range of 40–130°C, the mass loss of MPCM@PDA@Au silk fabrics was reduced compared to unmodified silk fabrics due to the protective effect of the polyurethane layer. In addition, when the temperature was increased to 350–480°C, the mass loss mainly originated from the thermal decomposition of PMMA.[46] Notably, n-octadecane, which was used in this study, effectively retarded the thermal loss of PMMA by being encapsulated in its outer wall, thus significantly enhancing the stability of the material. More critically, the degradation temperature of the MPCM@PDA@Au silk fabric is much higher than the normal use temperature of phase change fabrics, making it very suitable for the preparation and application of phase change fabrics.

The temperature responses of untreated silk fabrics, silk fabrics treated only with waterborne polyurethane (WPU), and silk fabrics modified with different concentrations of phase change capsules were compared under near-infrared light (wavelength 808 nm, light power 0.134 W/cm²). Observed by infrared thermography, the results are shown in Figure 5A–E The silk fabric

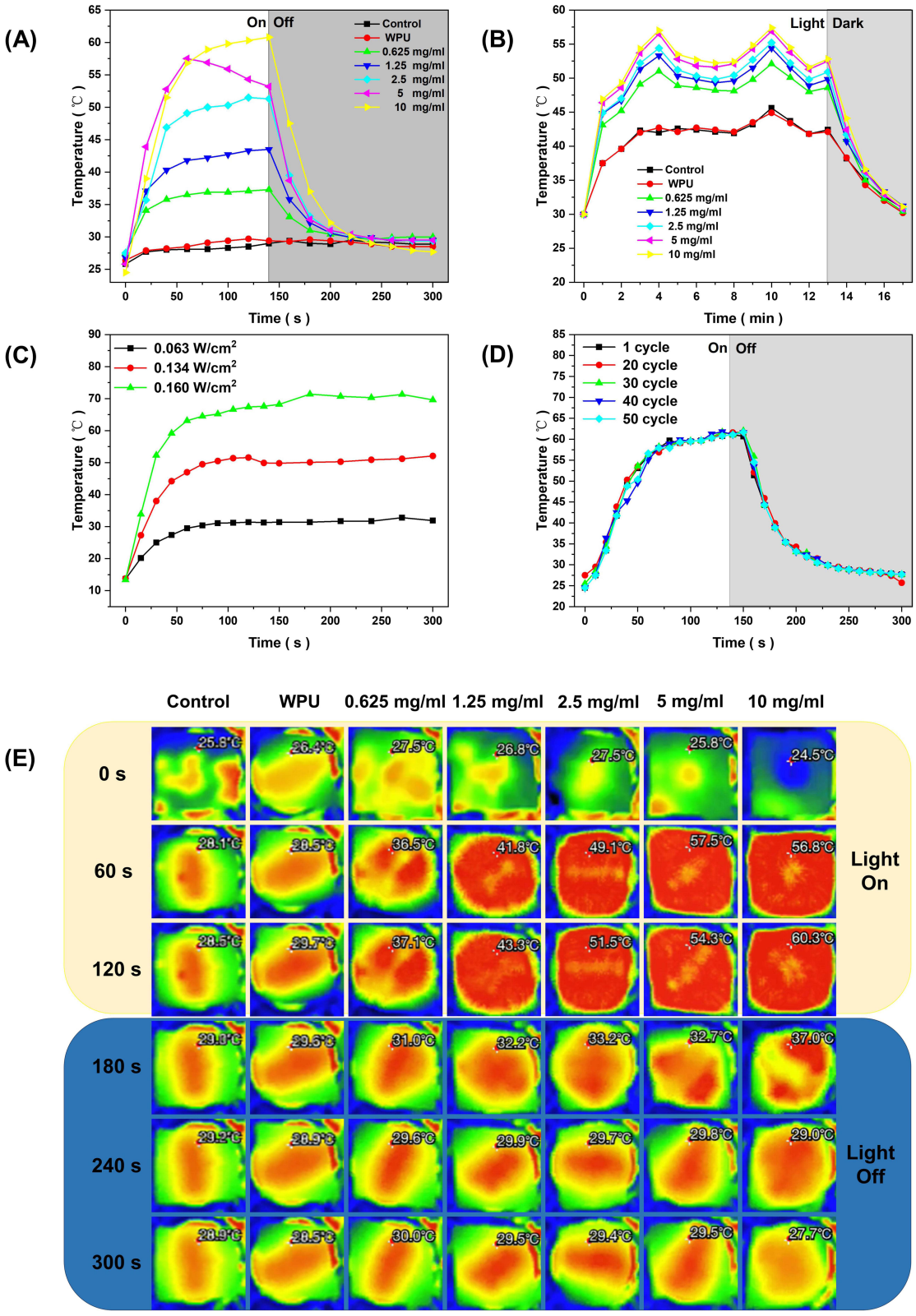

Figure 5 Comparison of the heating rate of photothermal fabrics under (**A**) NIR light and (**B**) solar light. (**C**) Comparison of the rate of photothermal warming at different power levels. (**D**) Photothermal condition of fabrics heated five times repeatedly under near-infrared light. (**E**) Infrared images of fabrics heated by near-infrared light.

modified with MPCM@PDA@Au rapidly warmed up from room temperature of 25 °C to 60 °C in 50s, demonstrating excellent photothermal conversion efficiency. It is worth mentioning that when the light source is switched off, its temperature does not drop sharply, but falls back gently, which indicates that MPCM@PDA@Au silk fabric not only has high photothermal conversion efficiency, but also can effectively store and slowly release heat. These silk fabric samples were further tested under natural light conditions. As shown in Figure 5B, the MPCM@PDA@Au modified silk fabrics rapidly increased from the outdoor temperature of 30°C to 57°C in just 4 minutes, which once again confirmed their excellent photothermal performance. MPCM@PDA@Au silk fabrics exhibited excellent photothermal performance, which was mainly attributed to the potent light absorption and heat conversion ability of dopamine. In addition, the gold nanoparticles modified on the surface of MPCM@PDA@Au also possessed significant photothermal properties, which further enhanced the photothermal conversion ability of the silk fabric and made it outstanding in this field.[47,48] In order to investigate the effect of light power on the photothermal performance of MPCM@PDA@Au silk fabrics, modified silk fabrics with a concentration of 5 mg/mL were selected and experiments were carried out at three light powers of 0.063 W/cm², 0.134 W/cm² and 0.160 W/cm². The results are shown in Figure 5C, with the increase of light power, the heating rate and final temperature of silk fabrics were significantly increased. Finally, the reusability of MPCM@PDA@Au silk fabrics was tested. It was irradiated several times under a near-infrared light source of 0.134 W/cm² and the temperature change was recorded by an infrared thermal imager. As shown in Figure 5D, the photothermal properties of the silk fabric remained almost unchanged after fifty consecutive cycles, demonstrating the excellent reusability of the MPCM@PDA@Au silk fabric. These results provide strong support for the application of MPCM@PDA@Au silk fabric in the fields of photothermal conversion and thermal energy storage, demonstrating its broad application prospects in many fields.

In order to deeply investigate the heat storage and exothermic properties of MPCM@PDA@Au silk fabrics, the present study employed differential scanning calorimetry (DSC) to exhaustively test the silk fabrics treated with 10 mg/mL concentration of MPCM@PDA@Au. The test results, as shown in Figure 6, clearly revealed that the MPCM@PDA@Au silk fabrics exhibited multiple significant exothermic peaks in the temperature range of 6.73–21.81 °C, while a distinctive heat-absorbing peak was observed in the temperature interval of 24.83–34.35 °C. As shown in the Table 1, the enthalpy of melting and crystallisation of MPCM@PDA@Au silk fabrics were as high as 41.58 J/g and 43.3 J/g, respectively, which fully proves that MPCM@PDA@Au silk fabrics possess excellent heat storage and exothermic capabilities. In view of its excellent thermal performance, MPCM@PDA@Au silk fabric shows a broad application prospect in the field of personal thermal management.

In order to assess the effect of different treatments on the bacteriostatic properties of silk fabrics, untreated silk fabrics, silk fabrics treated with waterborne polyurethane (WPU), and silk fabrics modified with phase change capsules (MPCM@PDA@Au) were compared. In the experiment, these fabrics were made into circular samples with a diameter

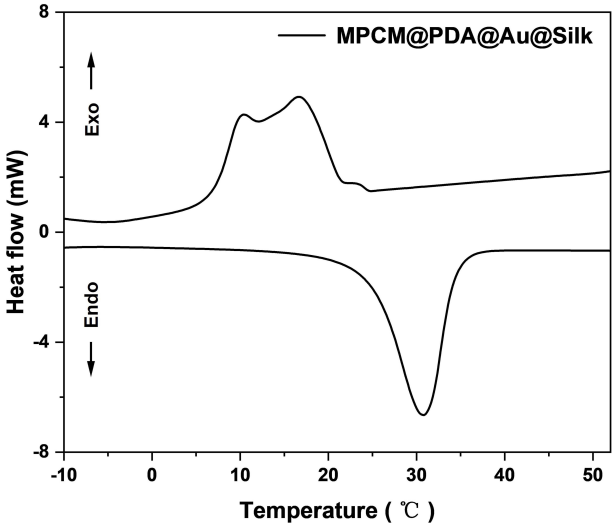

Figure 6 Crystallizing and melting DSC curves of MPCM@PDA@Au silk fabrics.

Table 1 Phase Change Properties of MPCM@PDA@Au Silk Fabrics

	T_m(°C)	T_s (°C)	ΔH_m(J/g)	ΔH_s(J/g)
MPCM@PDA@Au@Silk	30.85	16.48	41.58	43.3

of 6.0 mm and placed in a medium containing E. coli and S. aureus, and incubated at 37°C for 24 h. The results are shown in Figure 7. The bacteriostatic effect of each sample was assessed by observing the size of the inhibition circle. The results showed that both untreated silk fabrics and silk fabrics treated only with waterborne polyurethane did not exhibit significant bacteriostatic effects against E. coli and S. aureus. However, it is encouraging to note that silk fabrics modified with MPCM@PDA@Au produced significant circles of inhibition in the culture media of both bacteria. Specifically, the diameter of the inhibition circle reached 12.6 mm in the medium of E. coli and 10.1 mm in the medium of S. aureus. These results strongly demonstrated that the MPCM@PDA@Au-modified silk fabrics had excellent bacterial inhibition effects on E. coli and S. aureus.

Experimental Method

Materials

Silk fabric (19 mM, density: 114 g/m^2) was purchased from Ningbo Yunling Textile Trading Co. n-octadecane, sodium dodecyl sulphate (SDS), methyl methacrylate (MMA), Dopamine hydrochloride were purchased from Aladdin Reagent Co. waterborne polyurethane (WPU), analytically pure were purchased from Xilong Science Co. Pentaerythritol tetraacrylate (PETRA) was purchased from Shanghai Macklin Biochemical Ltd., LB broth agar was purchased from Shanghai Sangong Bioengineering Co. Ltd, Staphylococcus aureus and Escherichia coli were supplied by the Institute of Sericulture, Chinese Academy of Agricultural Sciences, plug-in thermal imager (312-Z5mini) was purchased from Shenzhen Chuangzhifei Technology Co., Ltd, 808nm NIR LEDs (10W, 20W, 30W) were purchased from Shenzhen Fangpu Optoelectronics Co.

MPCM Synthesis

As shown in the process of scheme 1A, a quantitative amount of n-octadecane was first mixed with a small amount of sodium dodecyl sulphate (SDS) and dissolved in deionised water. To ensure that the two substances were completely dissolved, a water bath heating method was used to precisely control the solution temperature at 35°C. Subsequently, the solution was stirred at high speed for a continuous period of 30 min using a homogeniser at up to 15,000 rpm to ensure that the solution was well mixed and formed a stable emulsion. Next, the prepared emulsion was placed in a flask along

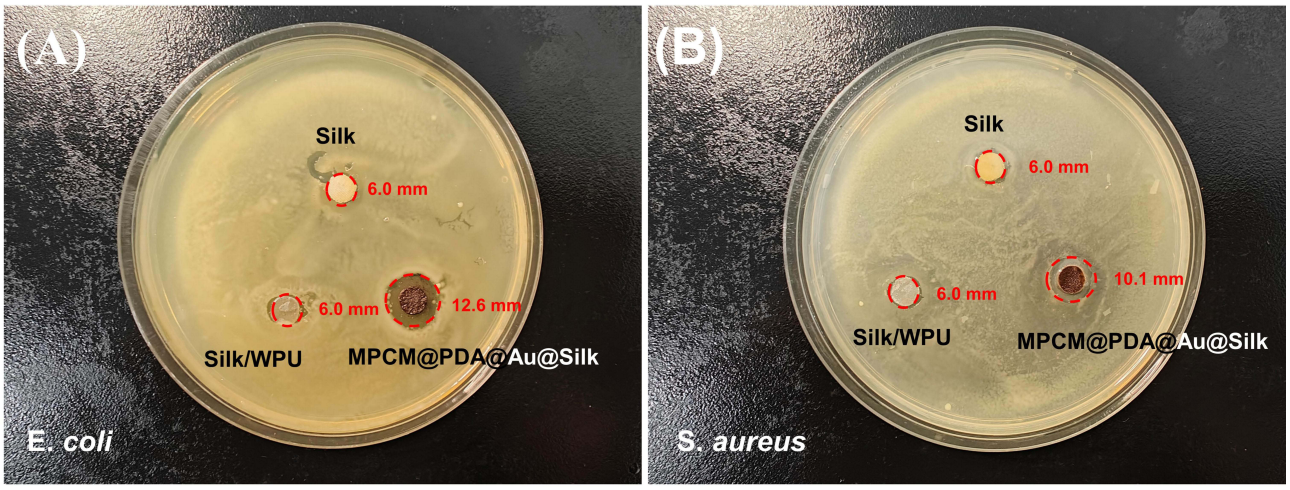

Figure 7 Pictures of the size of the circle of inhibition of untreated silk fabrics, silk fabrics treated with waterborne polyurethane (WPU), and silk fabrics modified with phase change capsules (MPCM@PDA@Au). (**A**) E. coli and (**B**) S. aureus.

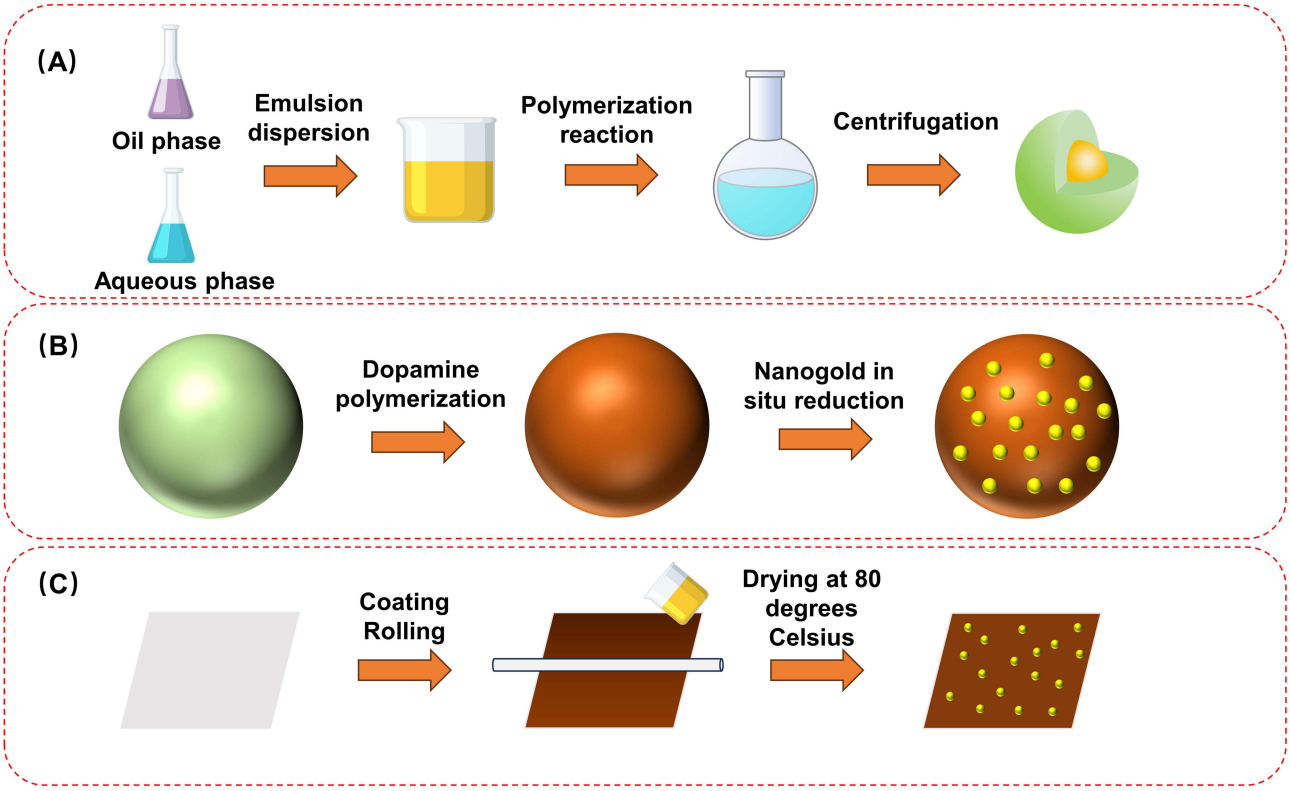

Scheme 1 (**A**) Depicts the synthesis procedure of MPCM. (**B**) Illustrates the modification process of MPCM@PDA@Au. (**C**) Outlines the preparation of MPCM@PDA@Au silk fabrics.

with methyl methacrylate (MMA), pentaerythritol tetraacrylate (PETRA), and the initiator azobisisobutyronitrile (AIBN). The reaction was carried out at a constant temperature of 85 °C in a water bath for up to 6 hours with a stirring speed of 600 rpm to ensure that the reaction proceeded adequately. At the end of the reaction, high-speed centrifugation was employed to successfully separate the MPCM from the reaction solution. This well-designed preparation process not only ensured the precise preparation of MPCM, but also greatly improved the production efficiency. Through a series of meticulous operation steps, the preparation of MPCM was ensured to be precise, reliable, efficient and convenient.

MPCM@PDA@Au Synthesis

As illustrated in the process diagram of scheme 1B, an amount of MPCM was accurately weighed and added to a 2 g/L aqueous solution of dopamine that had been adjusted to pH 8.5 with Tris-HCl. The mixture was stirred continuously for 24 h at room temperature to ensure that the reaction proceeded adequately. Upon completion of the reaction, MPCM@PDA was effectively separated from the mixture using high-speed centrifugation. Next, the obtained MPCM@PDA was homogeneously dispersed in chloroauric acid solution at concentrations of 0.03%, 0.07%, 0.1%, 0.15%, 0.2%, and 0.2%, respectively, and continued to be stirred for 4 h under room temperature conditions. After the reaction was completely finished, high speed centrifugation was again used to separate the MPCM@PDA@Au particles from the reaction solution. Finally, these particles were placed in an oven for drying process to finally obtain the desired MPCM@PDA@Au composites.

Preparation of MPCM@PDA@Au Silk Fabric

As illustrated in the process diagram of scheme 1C, in order to prepare MPCM@PDA@Au silk fabrics, firstly, the silk fabrics were immersed in a 7 mg/mL Na_2CO_3 solution and boiled to thoroughly remove the oil from their surfaces. After careful cleaning, the fabric blocks were precisely cut into 4×4 cm^2 sizes for subsequent use. Next, MPCM@PDA@Au particles were mixed with waterborne polyurethane solution (WPU) at a concentration gradient of 0.625 mg/mL, 1.25 mg/mL, 2.5 mg/mL, 5 mg/mL, and 10 mg/mL to form a series of solutions of different concentrations. Then, pre-

treated silk fabric blocks were immersed into these corresponding concentrations of waterborne polyurethane solution (WPU), respectively. To ensure that the particles were evenly distributed on the surface of the silk fabrics, a glass rod was used to gently press the surface of the fabric blocks. Finally, the impregnated silk fabrics were placed in an oven and dried at 80°C for 30 min to fully cure the waterborne polyurethane solution (WPU). After this series of careful treatment, the MPCM@PDA@Au silk fabric was successfully prepared.

Characterisation

Transmission electron microscopy (TEM) was used to observe the nanomorphology, and a certain amount of nanoparticles were dispersed in a certain volume of anhydrous ethanol solution and ultrasonically dispersed for 30 min, and then a trace amount of the solution was taken with a pipette gun and dropped on a copper mesh, and then dried in air. After drying, they were put into the equipment for characterisation. Scanning electron microscope (SEM) was used to analyse the surface morphology of microcapsule particles and silk fabric. In addition, the surface of silk fabric was scanned for elements using energy spectroscopy (EDS). X-ray diffraction (XRD) was used to analyse the physical phase of the nanomaterials, and the nanoparticle samples were poured into slides and then flattened with a glass slide by dropping alcohol, in which the metal target used was a Cu target with Kα rays; the scanning angle ranged from 10° to 80°; the scanning rate was: 5°/min; and the step angle was 0.02°. The chemical structure of microcapsule particles and silk fabric was observed by infrared spectroscopy (FTIR), and the infrared spectra were measured by taking a trace sample and adding a small amount of potassium bromide, and then drying and grinding the sample in the oven to form a very thin film for pressing and processing, and measuring the infrared spectra in a dry environment. The infrared spectra were measured in the band 4000cm^{-1}-400cm^{-1} with a resolution of 4cm^{-1} and a cumulative scan of 256 times. UV-Vis-NIR absorption spectra of nanoparticles were used to test the absorption of nanoparticles in different light bands. A fixed amount of MPCM, MPCM@PDA and MPCM@PDA@Au were dispersed in ethanol, respectively, and ultrasonically dispersed for 30 min, then the nanodispersions were pipetted into quartz cuvettes with drops of the nanodispersions to determine their UV-Vis-NIR absorption spectra. Fabric thermal stability was tested using thermogravimetry (TG). Silk fabrics were cut into pieces and tested for thermal stability using a thermogravimetric analyser (NETZSCH STA-2500,) under nitrogen atmosphere. The sample mass was 6–8 mg, the temperature range was room temperature-800°C, the temperature increase rate was 10 K/min, and the flow rate of protective gas was 20 mL/min. The thermal energy storage and release behaviour of phase change nanocapsules was investigated using an oscillometric scanning calorimeter to determine the thermal performance parameters such as phase change temperature and enthalpy of phase change. The sample mass of 3–5 mg was tested under nitrogen atmosphere with a temperature rise and fall rate of 10 °C/min.

Photothermal Conversion Experiments

The temperature evolution characteristics of untreated silk fabrics, waterborne polyurethane (WPU)-treated silk fabrics, and silk fabrics modified with different concentrations of MPCM@PDA@Au were characterised by irradiating these silk fabric samples with near-infrared (NIR) light under a NIR light source with a light power of 0.134 w/cm^2. Subsequently, a thermal imager was used to accurately monitor and record the temperature evolution of each sample during the irradiation process.

Bacterial Inhibition Experiment

In order to evaluate the effect of different treatments on the antimicrobial properties of silk fabrics, inhibition circle experiments were conducted. Firstly, untreated silk fabrics, silk fabrics treated with waterborne polyurethane (WPU), and silk fabrics modified with MPCM@PDA@Au were prepared. Using a hole punch, these fabrics were prepared as circular samples with a diameter of 6 mm. Next, E. coli and S. aureus were inoculated into LB liquid medium and incubated in a shaker for 24 hours. Subsequently, the bacterial solution was diluted 100 times and the fabric was evenly coated on the plate medium. The prepared circular fabric samples were placed on the media coated with the bacterial solution and incubated together for 24 hours. During this period, the formation of the ring of inhibition around the fabric was closely observed. At the end of the experiment, by comparing the size of the antibacterial circles around different fabrics, the enhancement effect of each treatment on the antibacterial performance of silk fabrics could be visually assessed.

Conclusions

In this study, a phase change microcapsule with n-octadecane as the core and poly(methyl methacrylate) (PMMA) as the shell layer was successfully synthesised, and gold nanoparticles were generated in situ on the surface of the microcapsule through the mediating effect of poly(dopamine), resulting in the innovative preparation of MPCM@PDA@Au composite microcapsules. In order to verify the structure and properties, various advanced characterisation techniques, such as scanning electron microscopy (SEM), transmission electron microscopy (TEM) and infrared spectroscopy (FTIR), were employed to fully confirm the successful preparation and effective modification of the MPCM@PDA@Au composite microcapsules. Subsequently, in this study, aqueous polyurethane was used as a medium to modify MPCM@PDA@Au microcapsules on the surface of silk fabric. In order to verify the modification effect, the successful modification of MPCM@PDA@Au on the surface of silk fabrics was further strongly demonstrated by scanning electron microscopy (SEM), energy spectroscopy (EDS), infrared spectroscopy (FTIR), and X-ray diffraction (XRD) characterisation. Differential scanning calorimetry (DSC) analyses and multiple photothermal experiments were carried out to fully evaluate the performance of the MPCM@PDA@Au silk fabric. The results show that the silk fabric not only possesses certain heat storage and exothermic capabilities, but also exhibits excellent photothermal conversion performance and good durability, demonstrating its great potential for application in the field of smart wearable and personal thermal management. In addition, thermogravimetric (TG) analyses show that the thermal degradation temperature of the MPCM@PDA@Au silk fabric is much higher than its normal use temperature, thus ensuring the fabric's thermal stability in practical applications. The bacterial inhibition experiments also further revealed that the silk fabric had a certain inhibitory effect on common bacteria such as E. coli and S. aureus, demonstrating good antimicrobial properties. In summary, the MPCM@PDA@Au silk fabric prepared in this study not only has the advantages of low cost and environmental protection, but also shows important application prospects in the field of smart wearable and personal thermal management. The successful development of this functional silk fabric provides new research ideas and development directions for future smart textiles and personal thermal management systems, and is expected to promote further innovation and development in related fields.

Disclosure

The authors report no conflicts of interest in this work.

References

1. Zhang X, Liu C, Shen C, et al. Promising commercial fabrics with radiative cooling for personal thermal management. *Sci Bull*. 2022;67(3):229–231. doi:10.1016/j.scib.2021.08.019
2. Xie X, Liu Y, Xu Z, et al. Silver coated textile for versatile personal thermal management via multi-order reflections. Research Square;2021.
3. Liu X, Zhang W, Zhang X, et al. Transparent ultrahigh-molecular-weight polyethylene/MXene films with efficient UV-absorption for thermal management. *Nat Commun*. 2024;15(1):3076. doi:10.1038/s41467-024-47432-z
4. Feng M, Feng S, Liu C, et al. Integrated passive cooling fabrics with bioinspired perspiration-wicking for outdoor personal thermal management. *Composites Part B*. 2023;264:110875.
5. Yang R, Xie F, Li Y, et al. Advancing thermal comfort: an innovative SiO2 microsphere-decorated shish-kebab film composite for enhanced personal cooling. *Adv Nanocomposites*. 2024;1(1):86–93. doi:10.1016/j.adna.2024.02.001
6. Cin ZI, Teke AC, Bedeloglu Z, et al. Development of thermo-regulating fabrics with enhanced heat dissipation via graphene-modified n - octadecane microcapsules. *Polym Eng Sci*. 2022;62(AC):210–219. doi:10.1002/pen.25845
7. Ramaiah G, Asfaw D, Mekonnen S, et al. Shear thickening fluids, nano-polymer materials and their application methods for textile substrates. *Mater Scie Forum*. 2022;1073:81–90. doi:10.4028/p-223rg7
8. Liu YLL, Zhang X, Ji J, Wu Y, Liu L. A review on thermal properties improvement of phase change materials and its combination with solar thermal energy storage. *Energy Technology: Generation, Conversion, Storage, Distribution*. 2021;9(7). doi:10.1002/ente.202100169
9. Bao Y, Guo R, Ge X, et al. Enhanced thermal insulation performance of polyethylene glycol-based polyurethane/W-doped VO2 composite phase change coating. Progress in organic coatings. *Int Rev J*. 2023;180:107574.
10. Su Y, Fan Y, Ma Y, et al. Flame-retardant phase change material (PCM) for thermal protective application in firefighting protective clothing. *Int J Ther Sci*. 2023;185:108075. doi:10.1016/j.ijthermalsci.2022.108075
11. Deng G, Yao L, Chen M, et al. The photothermal conversion and UV resistance of silk fabrics being achieved through surface modification with C@SiO2 nanoparticles. *Molecules*. 2023;28(24):7970. doi:10.3390/molecules28247970
12. Ren Y, Zhou R, Yang R, et al. Systematic review of material and structural design in interfacial solar evaporators for clean water production. *Solar RRL*. 2023;7(5):2201014. doi:10.1002/solr.202201014
13. Saerona K, Cheol KH, Chun C, et al. Solar energy driven C–C bond cleavage in a lignin model compound with a D–π–A organic dye-sensitized photoanode. *Sustainable Energy Fuels*. 2023;7(10):2339–2348.

14. Mishra S, Ghatak SR, Swain SC et al. Loss reduction and improvement of voltage profile in a three phase unbalanced distribution system using intermittent solar power resource, F.In2020 International Conference on Renewable Energy Integration into Smart Grids: A Multidisciplinary Approach to Technology Modelling and Simulation (ICREISG);2020.
15. Li J, Chang Q, Xue C. Carbon dots efficiently enhance photothermal conversion and storage of organic phase change materials through interfacial interaction. *Carbon: Int J Sponsored by the Am Carbon Soc*. 2023;203:21–28.
16. Liu C, Wan Y, Gao Y. Polypyrrole-coated expanded graphite-based phase change materials for photothermal energy storage. *Mat Today Nano*. 2023;24:100432. doi:10.1016/j.mtnano.2023.100432
17. Jin L, Tan Y, Yuan S, et al. Phytic acid–decorated κ-carrageenan/melanin hybrid aerogels supported phase change composites with excellent photothermal conversion efficiency and flame retardancy. *Renewable Energy*. 2023;206:148–156. doi:10.1016/j.renene.2023.02.030
18. Xiang B, Zhang R, Zeng X, et al. An easy-to-prepare flexible dual-mode fiber membrane for daytime outdoor thermal management. *Adv Fiber Materials*. 2022;4(5):1058–1068. doi:10.1007/s42765-022-00164-5
19. Sun Z, Shi T, Wang Y, et al. Hierarchical microencapsulation of phase change material with carbon-nanotubes/polydopamine/silica shell for synergistic enhancement of solar photothermal conversion and storage. *Solar Energy Materials and Solar Cells: Int J Devoted to Photovoltaic, Photothermal, and Photochemical Solar Energy Conversion*. 2022;236:111539. doi:10.1016/j.solmat.2021.111539
20. Rakhimova G, Stolboushkin A, Vyshar O, et al. Strong structure formation of ceramic composites based on coal mining overburden rocks. *J Compos Sci*. 2023;7(5):209. doi:10.3390/jcs7050209
21. Gao G, Zhang T, Jiao S, et al. Preparation of reduced graphene oxide modified magnetic phase change microcapsules and their application in direct absorption solar collector. *Solar Energy Mater Solar Cells*. 2020;216:110695. doi:10.1016/j.solmat.2020.110695
22. Huang D, Wang Z, Sheng X, et al. Bio-based MXene hybrid aerogel/paraffin composite phase change materials with superior photo and electrical responses toward solar thermal energy storage. *Solar Energy Materials and Solar Cells: Int J Devoted to Photovoltaic, Photothermal, and Photochemical Solar Energy Conversion*. 2023;251:112124.
23. Weng M, Su J, Lin J, et al. Intrinsically lighting absorptive PANI/MXene aerogel encapsulated PEG to construct PCMs with efficient photothermal energy storage and stable reusability. *Solar Energy Materials and Solar Cells: Int J Devoted to Photovoltaic, Photothermal, and Photochemical Solar Energy Conversion*. 2023;254:112282. doi:10.1016/j.solmat.2023.112282
24. Kazaz O, Karimi N, Kumar S, et al. Heat transfer characteristics of fluids containing paraffin core-metallic shell nanoencapsulated phase change materials for advanced thermal energy conversion and storage applications. *J Mol Liq*. 2023;385:122385.
25. Kapoor S, Kundu SC. Silk protein-based hydrogels: promising advanced materials for biomedical applications. Acta biomaterialia. 2016;31:17–32.
26. Liu J, Ge X, Liu L, et al. Challenges and opportunities of silk protein hydrogels in biomedical applications. *Mater Adv*. 2022;3(5):2291–2308.
27. Zheng H, Zuo B. Functional silk fibroin hydrogels: preparation, properties and applications. *J Mat Chem B*. 2021;9(5):1238–1258. doi:10.1039/D0TB02099K
28. Pan S, Zhu M. Nanoprocessed silk makes skin feel cool. *Adv Fiber Materials*. 2022;4(3):319–320. doi:10.1007/s42765-022-00168-1
29. Wang W, Li M, Huang X, et al. Structural evolution mechanisms of Polydopamine/CdS and photothermal effect boosted photocatalytic H2 production activity. *Appl Surf Sci: J Devoted to the Properties of Interfaces in Relation to the Synthesis and Behaviour of Materials*. 2022;601:154114.
30. Huang X, Alva G, Jia Y, Fang G. Morphological characterization and applications of phase change materials in thermal energy storage: a review. *Renewable Sustainable Energy Rev*. 2017;72:128–145. doi:10.1016/j.rser.2017.01.048
31. Li P, Zou F, Wang X, et al. In-situ deposition preparation of n-octadecane@Silica@Polydopamine-doped polypyrrole microcapsules for photo-thermal conversion and thermal energy storage of full-spectrum solar radiation. *Solar Energy*. 2022;240:388–398.
32. Mohamed F, Ahmad MM, Hameed TA. Greener synthesis of lightweight, self-standing PMMA / CoFe 2 O 4 polymeric film for magnetic, electronic, and terahertz shielding applications. *Polym Adv Technol*. 2023;34(5):1497–1514. doi:10.1002/pat.5984
33. Hisham S, Tajuddin HA, Sarih NM, et al. Evaluation of thermal and physical properties of PMMA/PMVEMA-ES blends as organic coating. *Pigment Resin Technol*. 2023;52(1):82–90. doi:10.1108/PRT-09-2021-0108
34. Turki A, Bdaiwi W. The use of pistachio shell was residues to reinforce the PMMA used in the bases of dentures. AIP conference proceedings, 2023, 2839(1). AIP Publishing;2023.
35. Dang Y, Xing CM, Quan M, et al. Substrate independent coating formation and anti-biofouling performance improvement of mussel inspired polydopamine. *J Mat Chem B*. 2015;3(20):4181–4190. doi:10.1039/C5TB00341E
36. Liu S, Qileng A, Huang J, et al. Polydopamine as a bridge to decorate monodisperse gold nanoparticles on Fe3O4 nanoclusters for the catalytic reduction of 4-nitrophenol. *RSC Adv*. 2017;7:45545–45551.
37. Zhang QZJ, Sheng Q, Zheng J. Preparation of tubular HNTs@PDA-Au nanocomposites and its electrocatalysis of hydrazine. *Nano: Brief Rep Rev*. 2018;13(2):1850019. doi:10.1142/S1793292018500194
38. Lee J, Park JC, Song H. A nanoreactor framework of a Au@SiO2 Yolk/Shell structure for catalytic reduction ofp-nitrophenol. *Adv. Mater*. 2008;20(8):1523–1528. doi:10.1002/adma.200702338
39. Ashrafi SJ, Yazdian F, Zaremi ASH, et al. Thermal distribution of silica coated gold nano rods in tissue-like phantom as in vitro model for plasmonic photo thermal therapy. *Biomed Pharmacol J*. 2016;9(3):1189–1201. doi:10.13005/bpj/1067
40. Cao J, Wang C. Multifunctional surface modification of silk fabric via graphene oxide repeatedly coating and chemical reduction method. *Appl. Surf. Sci*. 2017;405:380–388. doi:10.1016/j.apsusc.2017.02.017
41. Mohan R, Jineesh AG, Prabu NM. Fabrication of reusable polymer nanocomposite films made of thermoplastic polyurethane and modified BiVO_4 for photodegradation of Malachite Green. *Environ. Eng. Res*. 2022;27:4.
42. Akar A, Degirmenci B, Koken N. Fire-retardant and smoke-suppressant rigid polyurethane foam composites. *Pigment Resin Technol*. 2023;52(2):237–245.
43. Sivakumar P, Du SM, Selter M, et al. Improved adhesion of polyurethane-based nanocomposite coatings to tin surface through silane coupling agents. *Int J Adhes Adhes*. 2021;110:102948.
44. Banea MD, Da Silva LFM, Campilho RD. The effect of adhesive thickness on the mechanical behavior of a structural polyurethane adhesive. *J Adhes*. 2015;91(5):331–346.
45. Cai H, Gao L, Chen L, et al. An effective, low-cost and eco-friendly method for preparing UV resistant silk fabric. *J Nat Fibers*. 2021;19(13):5173–5185. doi:10.1080/15440478.2021.1875362

46. Yoshida DQZ. Size effect of silica nanoparticles on thermal decomposition of PMMA. *J Therm Anal Calorim*. 2010;99(1):21–26.
47. Dheyab MA, Aziz AA, Khaniabadi PM, et al. Gold nanoparticles-based photothermal therapy for breast cancer. *Photodiagn Photodyn Ther*. 2023;42(103312):103312. doi:10.1016/j.pdpdt.2023.103312
48. Zhang D, Yang A-S, Jiang Z, et al. Paraffin@ silica@ poly (dopamine)/Silver phase change microcapsules with efficient photothermal conversion performance. *Energy Fuels*. 2023;37(21):16951–16961.

International Journal of Nanomedicine Dovepress

Publish your work in this journal

The International Journal of Nanomedicine is an international, peer-reviewed journal focusing on the application of nanotechnology in diagnostics, therapeutics, and drug delivery systems throughout the biomedical field. This journal is indexed on PubMed Central, MedLine, CAS, SciSearch®, Current Contents®/Clinical Medicine, Journal Citation Reports/Science Edition, EMBase, Scopus and the Elsevier Bibliographic databases. The manuscript management system is completely online and includes a very quick and fair peer-review system, which is all easy to use. Visit http://www.dovepress.com/testimonials.php to read real quotes from published authors.

Submit your manuscript here: https://www.dovepress.com/international-journal-of-nanomedicine-journal